Available online at www.sciencedirect.com
SCIENCE DIRECT®
Journal of Nuclear Materials 337–339 (2005) 206–210
journal of nuclear materials
www.elsevier.com/locate/jnucmat

Simulation of afterglow plasma evolution in an inertial fusion energy chamber

B.K. Frolov [a,*], A.Yu. Pigarov [a], S.I. Krasheninnikov [a], R.W. Petzoldt [b], D.T. Goodin [b]

[a] UCSD Center for Energy Research, University of California at San Diego, EBU-II, 9500 Gilman Dr., La Jolla, CA 9209-0417, USA
[b] General Atomics, P.O. Box 85608, San Diego, CA 92186, USA

Abstract

The temporal evolution of plasma and gas parameters during the afterglow phase of cyclic operation of an inertial fusion-energy reactor chamber is simulated with a zero-dimensional code. The results of self-consistent modeling of plasma/gas cooling, plasma recombination, and the heat power load on a cryogenic fusion-fuel target are presented. The role of intrinsic impurity radiation and the edge plasma region in plasma cooling is analyzed. The impacts of large convective cells and large concentrations of a heavy-ion buffer gas inside the chamber on plasma evolution and target heat loads are discussed.

PACS: 52.55.Dy; 52.58.Ei; 52.25.Vy
Keywords: Edge plasma; Inertial fusion; Collisional-radiative model; Diffusion; Fusion reactor

1. Introduction

The cyclic operation of an inertial fusion energy (IFE) reactor requires safe delivery of fuel targets to the center of dry-wall chamber [1,2]. On its way, the cryogenic target has to move through the hot residual gas and plasma left from the previous shots [3,4]. As a result, the target experiences significant heating due to deposition of kinetic energy of plasma (q_{kp}) and gas (q_{kg}), release of plasma potential energy occurring as a result of plasma neutralization at the surface (q_{pot}), and absorption of radiation emitted by plasma (q_{rad}) and chamber walls (q_w). At the same time, cryogenic targets are very sensitive to the heat loading because it can severely deform the target surface violating the spherical symmetry requirements, so that effective target implosion becomes impossible. Recent analysis [1,2] of thermal and mechanical responses of targets to heat loadings has shown that the total flux should not exceed a critical level $q_{crit} \approx 1\,W/cm^2$. Higher flux levels of up to $10\,W/cm^2$ might be sustainable with reduced initial target temperature, for targets with outer insulating foam, or if some phase change from solid to liquid or gas is acceptable. However, as shown in Refs. [3,4], energy fluxes on the target surface associated with plasma, q_{kp} and q_{pot}, can be the dominant ones and exceed $10\,W/cm^2$ at the time $1/f_{tar}$, where $f_{tar} = 5–10\,Hz$ is the commercial range of target injection frequency. For plasma and atom densities $n_e = n_a = 10^{14}\,cm^{-3}$ and temperatures

* Corresponding author. Tel.: +1 858 822 4916; fax: +1 858 534 7716.
E-mail addresses: bfrolov@ucsd.edu (B.K. Frolov), apigarov@uscd.edu (A.Yu. Pigarov).

0022-3115/$ - see front matter © 2004 Elsevier B.V. All rights reserved.
doi:10.1016/j.jnucmat.2004.10.061

$T_e = T_a = 0.2\,eV$, $q_{pot} \approx 50$ and $q_{kp} \approx 3\,W/cm^2$ at 100 ms into the afterglow phase of the IFE operation cycle [4]. Therefore, strong recombination of plasma should occur in the chamber in order to bring the target heat loads below the critical value. In the paper we present the results of self-consistent modeling of plasma cooling, recombination, and target heating. The role of the edge plasma region is analyzed.

2. Edge plasma region in IFE chamber

In the absence of impurity radiation, the energy loss of deuterium–tritium (DT) bulk plasma is mainly due to electron heat conduction to the edge plasma region (EPR) in which recycling of neutral particles occurs. The characteristic width of EPR is determined by the depth of neutral atom penetration into plasma which is about the ionization length, λ_{ion}. Note, $\lambda_{ion} < 0.1\,m$ which is much less than chamber radius $R = 10\,m$, for $T_e \geqslant 3\,eV$ and $n_e \geqslant 10^{13}\,cm^{-3}$. For hot bulk-plasma, $\lambda_e/R > (m/M)^{1/2}$ (where $\lambda_e \propto T_e^2/n_e$ is the electron mean free path, m and M are the electron and ion masses), the electron temperature in the EPR is as high as the temperature T_0 at the chamber center. The ion temperature in this case can be higher than electron temperature, because bulk electrons are rapidly cooled by electron heat conduction, and only energy exchange with ions prevents electrons from cooling further down.

When electron temperature decreases so that $\lambda_e/R < (m/M)^{1/2}$, the high recycling regime (similar to that observed in tokamak divertors) occurs in the EPR. In this case, the electron-ion energy exchange rate exceeds the electron heat conduction rate, therefore, ion and electron temperatures equilibrate. Plasma temperature in the EPR, T_{EPR}, becomes much smaller than T_0 due to high collisionality. In fact, comparing the heat flux from the bulk plasma to the EPR, $q_{EPR} \approx n_e(T_0 - T_{EPR})(T_0/m)^{1/2}(\lambda_e/R)$, and the plasma energy deposition to the wall $q_w \approx \gamma_t n_e T_{EPR}(T_{EPR}/M)^{1/2}$ (where $\gamma_t \approx 8$ is the energy transmission coefficient through electrostatic sheath [4]), we obtain $T_0 \gg T_{EPR}$ if $\lambda_e/R < (m/M)^{1/2}$. Also, the pressure P is approximately constant across the chamber since the rate of pressure equilibration $\nu_p \approx (T_0/M)^{1/2}/R$ is greater than the cooling rate $\nu_{Te} \approx (\lambda_e/R)(T_0/m)^{1/2}/R$. We can assume that total number N of nuclei in the chamber is constant, i.e. there is no significant particle adsorption/release at the wall. An average nuclei density is $n_{res} = N/V$ (V is the chamber volume).

The following equation can be used to describe plasma cooling in the case where $\lambda_e/R < (m/M)^{1/2}$:

$$3n_e \partial T/\partial t = \nabla(\chi_{SH}\nabla T), \tag{1}$$

where χ_{SH} is the Spitzer–Harm (SH) thermal conductivity. The boundary conditions are $T(r = R) = 0$, $dT/dr(r = 0) = 0$. We search for a solution of Eq. (1) in the form $T(t,r) \equiv T_0(t)\theta(r)$, where $T_0(t)$ is the temperature at the plasma center, and $\theta(r)$ is the dimensionless radial profile. The assumptions of uniform pressure $P(t) = 2T(t)n_e(r)\theta(r)$ and constant N allow neglect of the convective terms and plasma density variation in Eq. (1). Then the solution of Eq. (1) is

$$T_0(t) = T_0(0)[1 + t/\tau_T]^{-2/5}, \quad \theta(r) = [1 - (r/R)^2]^{2/7}, \tag{2}$$

where $\tau_T = 0.7 n_{res} R^2/[b\chi_{SH}(T_0\ \ (0))]$, $b = (4\pi/V)\int dr r^2/\theta(r) \approx 0.5$. The corresponding flux to the edge region is $q_{EPR}(t) = (4/7)\chi_{SH}(T_0)\ T_0/R$. This solution holds while the ratio N_{EPR}/N is small (N_{EPR} is the number of nuclei in the EPR). Using (2), we obtain $N = (4/3)\pi\ R^3 P/T_0$ and $N_{EPR} = 4\pi R^2 \int [P/T] dx \approx 8\pi R^2 [P\chi_n(T_{EPR})/q_{EPR}]\,[E_{ion}/T_{EPR}]$, where $E_{ion} \approx 30\,eV$ is the amount of thermal energy lost by the plasma per ionization; and we replaced integration over the EPR width x by integration over the temperature by using the following estimation of temperature gradient. For $T_{EPR} \ll E_{ion}$, the energy delivered into EPR by flux q_{EPR} is mainly spent on the ionization of neutrals and only a small part $\vartheta_n = T_{EPR}/[T_{EPR} + E_{ion}]$ is conducted to the wall. The corresponding temperature gradient is $|dT/dx| \approx q_{EPR}\vartheta_n/\chi_n$, where χ_n denotes the neutral thermal conductivity. Finally we obtain $N_{EPR}/N \approx [14\chi_n(T_{EPR})E_{ion}]/[\chi_{SH}(T_0)T_{EPR}]$. For pure DT plasma, $T_{EPR} \approx 3\,eV$, the central temperature T_0 should exceed $T_{0*} \approx 10\,eV$ to satisfy $N_{EPR}/N < 1$.

Thus, the edge plasma region plays important role in temporal evolution of collisional plasma without impurities on the timescale $\geqslant \tau_T$. Typically, for $n_0 = 10^{15}\,cm^{-3}$ DT-plasma, the central temperature T_0 decreases from 100 eV to T_{0*} only in about 10 ms. When temperature of the afterglow plasma drops below T_{0*}, the edge region rapidly 'expands' since $N_{EPR} \to N$. The further evolution of plasma temperature and density is similar to that of plasma with a small amount of impurities. This is analyzed in Section 3.

3. Evolution of plasma with impurities

Even small amount of high-Z impurities (like intrinsic carbon) creates strong energy loss from bulk plasma due to line radiation at $T_0 > T_{0*}$, whereas impurity radiation becomes negligibly small when central temperature drops below T_{0*}. The density n_Z of impurities, which is required to radiate the amount $(4/3)\pi R^3 L_Z n_Z n_e$ of energy delivered by electron heat conduction $q_e = 4\pi R^2 n_e T_0 c_{s0}(\lambda_e/R)$, $c_{s0} \propto (T_0/m)^{1/2}$, is $n_Z \approx 3T_0\lambda_e c_{s0}/[R^2 L_Z]$, where $L_Z(T_0)$ is the radiation rate coefficient. For carbon impurity, $T_0 = T_{0*}$, $L_Z(T_{0*}) \approx 10^{-26}\,W cm^3$, $n_e = 10^{20}\,m^{-3}$, the radiation loss exceeds the conduction flux when $n_Z/n_e \geqslant 10^{-3}$. The impurity concentrations 10^{-3} to 10^{-2} are small in a sense that they do not affect collision

frequencies but they cause the cooling to occur in the entire chamber volume.

The following system of two coupled equations describes the temporal evolution of volume-averaged plasma density $n_e = n_i$ and temperature $T = T_i = T_e = T_a$ (see [4] for details):

$$\partial n_e/\partial t = -\Gamma_{tran} - (S_{rec} n_i - S_{ion} n_a) n_e, \quad (3)$$

$$3/2(n_{res} + n_i)\partial T/\partial t = 3/2T(S_{rec} n_i - S_{ion} n_a) n_e - W_{loss}, \quad (4)$$

where n_a is the atom density; $n_{res} = n_i + n_a$ is the residual density which is the number of nuclei per unit volume; n_{res} is assumed to be constant; S_{ion} and S_{rec} are the multi-step ionization and recombination rate coefficients; $W_{loss} = W_{tran} + (5/2)T\Gamma_{tran} + \Omega_{rec} n_e\ n_i + \Omega_{ion} n_e n_a + \Omega_Z n_Z n_e$; Ω_{rec} and Ω_{ion} are the rate coefficients for plasma kinetic energy loss associated with the multi-step recombination and ionization; Ω_Z is the plasma energy loss due to impurity radiation; n_Z is assumed to be a fixed fraction of n_{res}; $n_Z = \zeta_{imp} n_{res}$. The term Γ_{tran} describes the transport of plasma particles to the wall. In a diffusive approximation, we get the following expression: $\Gamma_{tran} = C_g D_A n_e/R^2$, where D_A is the ambipolar diffusion coefficient, and $C_g = \pi^2$ for spherical chamber. The plasma heat conduction loss term W_{tran} can be written as $W_{tran} = C_g(\kappa_e + \kappa_a)T/R^2$, where κ_e and κ_a are the SH electron and neutral thermal-conductivity coefficients, correspondingly. The system 3,4 is solved numerically for given initial values: $T(0) = T_0$ and $n_e(0) = n_{res}$. We use the Collisional Radiative Atomic Molecular Data (CRAMD) code [5] to calculate the rate coefficients: S_{rec}, Ω_{rec}, S_{ion}, Ω_{ion}, and Ω_Z as a function of plasma and gas parameters (n_e, n_a, T) and radius R which implicitly introduce the effects of multi-step excitation and plasma radiation re-absorption in the chamber. Based on the plasma/gas parameters, a standard plasma sheath model, the CRAMD data, and a realistic reflectivity data for radiation and particles from target surface [4], we calculate the peak total heat flux $q_{tot} = q_{pot} + q_{kp} + q_{kg} + q_{rad} + q_w$ and the time $\tau_{crit}(q_{crit})$ into afterglow phase which is required to reduce q_{tot} to acceptable level q_{crit}.

The main results obtained with plasma model (Eqs. (3) and (4)) are shown in Figs. 1–3. The typical temporal evolution of plasma density and temperature are given in Fig. 1 for DT plasma with $\zeta_{imp} = 1\%$ of carbon impurities and $R = 10$ m. As seen, for any n_{res} value, it takes roughly 1 ms for temperature to reach the 1 eV level mainly due to electron energy losses associated with ionization of neutrals and impurity radiation. Starting at about 1 eV, a weakly ionized gas cools predominantly by neutral heat conduction and the correspondent characteristic time τ_{cond} is, approximately, inversely proportional to n_{res}. As shown in Fig. 2, the non-radiative heat flux $q_{gp} = q_{kp} + q_{kg} + q_{pot}$ applied to the target surface

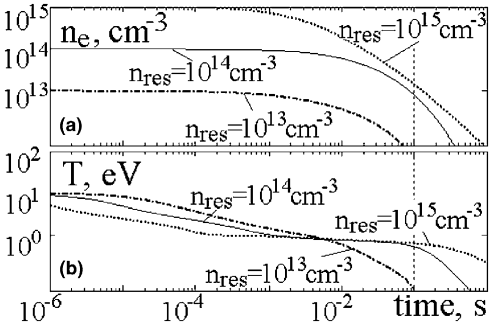

Fig. 1. The temporal evolution of (a) plasma density n_e and (b) temperature T. On each panel, the curves correspond to different values of residual gas density n_{res}.

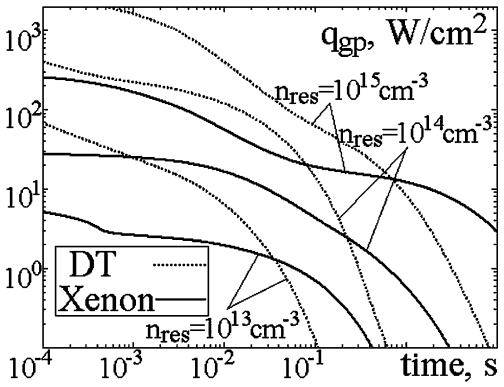

Fig. 2. The temporal evolution of non-radiative flux q_{gp} is given for DT and Xe residual gases. For each gas, three curves with different n_{res} values are shown.

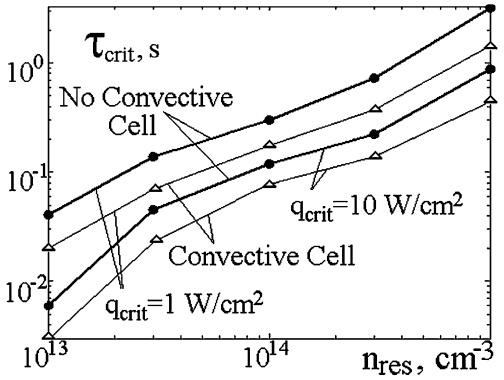

Fig. 3. The τ_{crit} times required to reduce the total heat flux q_{tot} to acceptable levels $q_{crit} = 1$ and 10 W/cm^2 are shown versus residual density n_{res} with and without convective cells.

decreases substantially on the same time-scale τ_{cond} in pure DT. At 100 ms, $q_{gp} < 1$ W/cm^2 is only for low resid-

ual gas densities, $n_{res} < 3 \times 10^{19}\,m^{-3}$. Fig. 3 illustrates that the higher n_{res} the longer is the time $\tau_{crit,total}$ necessary to reduce total heat load to acceptable level q_{crit}. The commercial frequency $f_{tar} = 5$–$10\,Hz$ is consistent with $\tau_{crit,total}$ ($1\,W/cm^2$) only for $n_{res} < 3 \times 10^{19}\,m^{-3}$. The tenfold increase in q_{crit} reduces τ_{crit} only three times at fixed n_{res}.

4. Evolution of heavy-ion plasma

A heavy-particle noble buffer gas is widely considered to soften the chamber wall response to the fusion blast [6]. However to fully accomplish this mission, the buffer gas pressure should be very large ($\geqslant 5\,Torr$). Compare the case when the chamber is filled with pure xenon to the pure DT case. The thermal velocity V_{Xe} of Xe is $\xi = (M_{Xe}/M_{DT})^{1/2} \approx 7$ times smaller than velocity V_{DT} of DT. This difference initially makes the particle and energy fluxes on the fuel target in Xe be ξ-times smaller than in DT, however, the plasma cooling becomes much slower as well. The neutral diffusivity $(D_n)_{Xe} \propto V_{Xe}/\sigma_{Xe}$ scales as $(D_n)_{Xe} \approx 0.07(D_n)_{DT}$, since $V_{Xe} = V_{DT}/\xi$ and $\sigma_{Xe} \approx 2\sigma_{DT}$, where σ_{Xe} and σ_{DT} are the cross-sections for Xe–Xe and D–T scattering. Heat conductivities follow the same scaling.

We simulate the temporal evolution of Xe and DT plasmas with model described by Eqs. (3) and (4). The calculated heat flux q_{gp} is shown on Fig. 2 for $R = 10\,m$. As seen, for given n_{res}, although the initial q_{gp} value is smaller in Xe, the heat flux in D–T decreases much faster in time than that in Xe. The reason is the smaller diffusivities of heavy gases and the faster recombination due to higher plasma densities in Xe. However, for densities $n_{res} > 10^{14}\,cm^{-3}$, q_{gp} exceeds $10\,W/cm^2$ at the end of afterglow phase $1/f_{tar} = 0.1$–$0.2\,s$ in both Xe and DT. If the critical flux $q_{crit} = 1\,W/cm^2$ and $f_{tar} = 5\,Hz$, then the usage of high-pressure buffer gas will be impossible because of predicted extreme heat loads.

Consider the hypothetical case when fuel targets can withstand heat loads $q_{crit} = 20$–$30\,W/cm^2$. As follows from Fig. 2, these high q_{crit} may be consistent with 10–30 mTorr of Xe in the chamber (even with an injection frequency of 15 Hz) that can provide a significant reduction of surface wall temperature rise and help to protect some important IFE components like mirrors for laser direct drivers [2].

5. Convective cells in IFE chamber

Plasma cooling is strongly affected by convective motion of plasma and gas, which effectively brings hot particles closer to the wall and enhances heat flux due to a reduced gradient length. As suggested in [3], only large convective cells (CC) with characteristic size of about chamber radius R can exist for a time comparable to $1/f_{tar}$, because viscosity effects quickly dissipate the smaller size modes of convective motion. The CC decay time is $\tau_{cc} = R^2/\pi^2 \nu_{vis} \approx 0.1\,s$, where $\nu_{vis} \approx 10^6\,cm^2/s$ is the typical value of kinematic viscosity. The large CC introduces toroidal symmetry of constant temperature and density contours instead of spherical symmetry considered above. For simplicity, we approximate the toroidal CC by two cylinders [3]. To maintain constant values of plasma/gas parameters along the flux surface, the tangential velocity V_R at the outer radius should be $V_R \geqslant 2\pi R_{cyl} f_{tar}\,300\,m/s$, $R_{cyl} = R/2$, and Reynolds number is $V_R R/\nu_{vis} \approx 30$.

To estimate diffusion time $\tau_D = 1/\gamma_D$, we solve the eigenvalue problem: diffusion equation $\nabla^2 n + k^2 n = 0$ with $dn/dr(r = 0) = 0$, $n(r = R) = 0$, where $k^2 = \gamma_D/D$, D is the diffusion coefficient. The solutions are Bessel functions: $j_0(kr)$ and $J_0(k_{cyl} r_{cyl})$, respectively, for spherical and cylindrical geometries. The boundary condition $n(r = R) = 0$ gives the following values: $k = \pi/R$, $k_{cyl} \approx 4.8/R$. Then, the ratio of diffusion times in the two different geometries is $(\gamma_D)_{cyl}/\gamma_D \approx (4.8/\pi)^2$, i.e. convective cells decrease almost twofold the diffusion time. The same conclusion applies to the heat conduction.

We use Eqs. (3) and (4) to simulate the plasma evolution with and without CC. The calculated τ_{crit} times necessary to attain acceptable levels $q_{crit} = 1$ and $10\,W/cm^2$ are plotted in Fig. 3 for DT gas, $R = 10\,m$, $\zeta_{imp} = 1\%$. As seen, convective cells decrease τ_{crit} twofold in a wide range of densities and q_{crit}.

6. Conclusions

We presented the results of self-consistent zero-dimensional modeling of plasma/gas cooling, plasma recombination, and the expected heat fluxes on a fuel target surface during the afterglow phase of an operational cycle of the IFE chamber. The results show that in the chamber of 10 m in radius the fuel-target injection frequency 6 Hz (which is required for an economic reactor) is consistent with acceptable peak heat flux of about $1\,W/cm^2$ only for gas low residual gas densities $n_{res} < 10^{20}\,m^{-3}$. Even small concentrations $\zeta_{imp} = 0.1$–1% of impurities allow rapid ($\sim 1\,ms$) reduction of the initial temperature to 1 eV, whereas the further cooling is due to slow ($\sim 100\,ms$) neutral heat conduction. The higher densities, $n_{res} = 10^{20}$–$10^{21}\,m^{-3}$ (e.g. due to high-Z buffer gas) lead to inadequate injection frequency 0.1–2 Hz. Theoretically, these densities can be acceptable for targets that withstand the elevated heat flux $\geqslant 10\,W/cm^2$. A large-scale convective motion organized inside the chamber is an effective way to speed up the plasma

cooling and recombination. Our results motivate more detailed studies for a dry-wall IFE chamber concept with minimal buffer gas protection.

Acknowledgment

The work was performed under the auspices of the US Department of Energy by UCSD under grant DE-FG02-04ER54739 and by General Atomics under contract N00173-02-C-6007.

References

[1] R.W. Petzoldt, D.T. Goodin, et al., Nucl. Fusion 42 (2002) 1351.
[2] J.D. Sethian et al., Fusion 43 (2003) 1693.
[3] S.I. Krasheninnikov, in: Proceedings 29th Eur. Conf. Plasma Phys. Contr. Fus., Montreux, Switzerland, vol. 26B (2002) O-4.05.
[4] A.Yu. Pigarov et al., Phys. Plasmas 11 (2004) 5130.
[5] A.Yu. Pigarov, Phys. Scr. T 96 (2002) 16.
[6] R.R. Peterson et al., Phys. Plasmas 9 (2002) 2287.